



UNIVERSITI PUTRA MALAYSIA

COLOSSAL MAGNETORESISTANCE OF $(La_{1-x}A_x)_{0.67}Ca_{0.33}MnO_3$ [A=Sn, Sm and Er] PEROVSKITE

ZOHRA ALI MOHAMED GEBREL

FSAS 2003 38

**COLOSSAL MAGNETORESISTANCE OF $(La_{1-x}A_x)_{0.67}Ca_{0.33}MnO_3$
[A=Sn, Sm and Er] PEROVSKITE**

ZOHRA ALI MOHAMED GEBREL

**MASTER OF SCIENCE
UNIVERSITI PUTRA MALAYSIA
2003**



**COLOSSAL MAGNETORESISTANCE OF $(La_{1-x}A_x)_{0.67}Ca_{0.33}MnO_3$ [A=Sn, Sm
and Er] PEROVSKITE**

By

ZOHRA ALI MOHAMED GEBREL

**Thesis Submitted to the School of Graduate Studies, Universiti Putra Malaysia,
in Fulfilment of the Requirements for the Degree of Master of Science**

July 2003



DEDICATIONS

**To Prof. Dr. Halim,
for his patience and guidance**

**To my late father, my mother for her love and support
To all my sisters and brothers for their love and concern.....
To my brother Moftah for his support and understanding.....**

To all my family and my friends



Abstract of thesis presented to the Senate of Universiti Putra Malaysia in fulfilment of the requirements for the degree of Master of Science

**COLOSSAL MAGNETORESISTANCE OF
(La_{1-x}A_x)_{0.6}Ca_{0.33}MnO₃ [A=Sn, Sm and Er] PEROVSKITE**

By

ZOHRA ALI MOHMED GEBREL

July 2003

Chairman: Professor Abdul Halim bin Shaari, Ph.D.

Faculty : Science and Environmental Studies

In this work, the colossal magnetoresistance (CMR) of (La_{1-x}Sn_x)_{2/3}Ca_{1/3}MnO₃ [LSnCMO], (La_{1-x}Sm_x)_{2/3}Ca_{1/3}MnO₃ [LSmCMO] and (La_{1-x}Er_x)_{2/3}Ca_{1/3}MnO₃ [LErCMO] ceramics samples, with x=0.0 to 0.4 were prepared by solid-state reaction technique. The structure, magnetic and electrical properties of the samples were investigated. The x-ray diffraction (XRD) spectrum for all the samples exhibit orthorhombic distorted and single-phase perovskite structures with the presence of some minor impurities. The magnetic properties were studied by measuring the susceptibility of the samples as a function of temperature at various magnetic fields. Ferromagnetic-paramagnetic phase transition temperature, T_c was determined for low doping concentration. The Curie temperature, T_c shifts to lower temperature as tin, samarium and erbium content was increased, indicating the loss of ferromagnetic order. For high tin content, the classical ferromagnetic order disappears and a cusp peak anomaly appears at 87 K, 68 K, 61 K and 55 K for x=0.1, 0.2, 0.3 and 0.4 respectively. The cusp shifts to higher temperature as the frequency increases from



125 Hz to 200 Hz and becomes sharper as magnetic field increases from 0.1 Oe to 10 Oe in agreement with spin glass behavior. However, LSmCMO system displays a classical ferromagnetic-paramagnetic transition for $x = 0.0, 0.01, 0.02$ and 0.04 and T_c shifts to lower temperature as samarium content increases. Also a cusp peak was observed at around 50 K for samples with $x \geq 0.03$. However, the study of frequency dependence of susceptibility did not show any shift in T_{cusp} . Thus the samples did not exhibit the spin glass behavior and T_{cusp} is called Néel temperature, T_N . In addition, LErCMO system also demonstrated that the samples with $x=0.01, 0.02$ and 0.03 exhibit the spin glass behavior and the respective spin-glass transition temperatures, T_{SG} are 99.7 K, 98.7 K and 70.5 K, respectively. But, samples with $x \geq 0.1$ did not show any ferromagnetic-paramagnetic transition at the range of 30 K to 300 K, possibly the Curie temperature for these samples is below 30 K. The pure sample, which exhibits T_c around 240 K and T_p around 200 K showed high level of porosity, and an average grain size of $3\mu\text{m}$. By replacing La with Sn, Sm and Er, respectively, in the LCMO system, the colossal magnetoresistance effect appear at low temperature and the highest value of CMR effect was observed at temperature approaching T_p . The highest CMR value was observed in LErCMO system with $x=0.03$ at 170 K. The value is 51 %. In LSnCMO, the maximum CMR value is 49 % at 200 K for the sample with $x=0.01$. While in the LSmCMO system the highest CMR value is displayed at 200 K for the sample with $x=0.02$.

Abstrak tesis yang dikemukakan kepada Senat Universiti Putra Malaysia sebagai memenuhi keperluan untuk ijazah Master Sains

**MAGNETORINTANGAN RAKSAKSA BAGI
(La_{1-x}A_x)_{0.67}Ca_{0.33}MnO₃ [A=Sn, Sm and Er] PEROVSKITE**

Oleh

ZOHRA ALI MOHAMED GEBREL

Julai 2003

Pengerusi : Profesor Abdul Halim Shaari, Ph.D.

Fakulti : Sains dan Pengajian Alam Sekitar

Dalam kajian ini, magnetorintangan raksasa bagi sampel seramik (La_{1-x}Sn)_{2/3}Ca_{1/3}MnO₃ [LSnCMO], (La_{1-x}Sm)_{2/3}Ca_{1/3}MnO₃ [LSmCMO], (La_{1-x}Er)_{2/3}Ca_{1/3}MnO₃ [LErCMO], dengan x=0.0 hingga 0.4 telah disediakan menggunakan teknik tindakbalas keadaan pepejal. Struktur, sifat magnet dan sifat elektrik bagi sampel tersebut telah dikaji. Spektrum belauan sinar-x bagi semua sampel menunjukkan orthorombik tercangga dan struktur perovskite fasa tunggal dengan kehadiran bendasing. Sifat magnet telah dikaji menggunakan ketelapan sebagai fungsi suhu pada medan magnet yang berbeza. Suhu peralihan fasa feromagnet-paramagnet, T_c telah ditentukan bagi kepekatan dopan yang rendah. Suhu Curie, T_c teranjak ke suhu yang rendah apabila kandungan timah, samarium dan erbium bertambah, yang menunjukkan kehilangan tertib feromagnet. Bagi kandungan timah yang tinggi, klasik tertib feromagnet hilang dan kejanggalan juring puncak masing-masing muncul pada 87 K, 68 K, 61 K dan 55K bagi x=0. 1, 0.2, 0.3



dan 0.4. Anjakan juring kepada suhu tinggi berlaku apabila frekuensi meningkat dari 125 Hz ke 200 Hz dan menjadi tajam semasa medan magnet meningkat dari 0.1 Oe ke 10 Oe dalam persetujuan dengan sifat spin kaca. Walau bagaimanapun, LSmCMO sistem, menunjukkan klasik ferromagnet-paramagnet bagi $x=0.0, 0.01, 0.02$ dan 0.04 dan T_c beranjak ke suhu yang rendah apabila kandungan samarium meningkat. Juga puncak juring pada sekitar 50 K diperhatikan bagi sampel dengan $x \geq 0.03$ dan kajian kebergantungan terhadap frekuensi bagi susceptibiliti tidak menunjukkan sebarang perubahan dalam T_{cusp} . Oleh itu, sampel tersebut tidak menunjukkan sifat spin kaca dan T_{cusp} adalah sebagai suhu Neel, T_N . Sebagai tambahan LErCMO sistem telah menunjukkan sampel dengan $x=0.01, 0.02$ dan 0.03 . mempamerkan sifat spin kaca dan masing-masing T_{SG} adalah 99.7 K, 98.7 K dan 70.5 K. Tetapi sampel dengan $x > 0.1$ tidak memperlihatkan sebarang ferromagnet-paramagnet pada julat 30 K ke 300 K. Kemungkinan suhu Curie bagi sampel ini di bawah 30 K. Sampel tulen, yang menunjukkan T_c sekitar 240 K dan T_p sekitar 200 K mempamerkan paras porositi yang tinggi, dan purata saiz butiran 3 μm . Dengan menggantikan La dengan Sn, Sm dan Er dalam magnetorintangan perovskite bagi LCMO sistem, purata magnetorintangan raksasa timbul pada suhu rendah dan kesan magnetorintangan yang besar telah diperolehi pada suhu mencapai T_p . Nilai CMR tertinggi diperhatikan dalam LErCMO sistem dengan $x=0.03$ ada 170 K dan nilai tersebut adalah 51%. Dalam LSnCMO, nilai maksimum CMR adalah 49% pada 200 K bagi sampel $x=0.01$. Walau bagaimanapun, sistem LSmCMO menunjukkan nilai CMR tertinggi pada 200 K bagi sampel dengan $x=0.02$.



ACKNOWLEDGEMENTS

I have enjoyed my time at the Universiti Putra Malaysia tremendously. Without its library and lab facilities, the research would be impossible to complete. I also benefited greatly from access to the facilities at this university.

First and foremost, I would like to express my utmost appreciation to my supervisor, Professor Dr. Abdul Halim Shaari not only for his great guidance, advice, discussions but also for his foresight to investigate new projects, which has always been the power that pushes our lab moving forward. For the past years it has been proved that, in most cases, I was getting confused and I am really grateful for his kindness and forgiveness. His patience and persistence in pursuing perfection has a great influence in my work. Second I would like to express my gratitude to Associate Professor Dr. Zainal Abidin Talib and Associate Professor Dr. Hishamuddin Zainuddin for their comments and suggestions throughout the research work and for taking the time to read my thesis during the long days, and proving me with comments that have significantly improved this thesis.

I would like to thank all the lecturers in the physics department for their comments and discussions. I also specifically thank Mr. Razak Harun for his technical favors and his assistance, and other staff in the physics department for their kind help.

Working with other graduate students in our lab was also a wonderful experience for me. First I would like to acknowledge all my colleagues who I worked



with them in this lab; especially Imad Hamadneh, Ifetan Ahmed, Abdullah Chik, Lim Kean Pah, Sharmiwati and Walter Charlos.

Last but not least, I would like to send all my love to my whole family, specifically my great mother who encourage me till I reached this position.



I certify that an Examination Committee met on 23/7/2003 to conduct the final examination of Zohra Ali Mohamed Gebrel on her Master of Science thesis entitled "Colossal Magnetoresistance of $(La_{1-x} A_x)_{0.67} Ca_{0.33} MnO_3$ [A=Sn, Sm and Er] perovskite" in accordance with Universiti Pertanian Malaysia (Higher Degree) Act 1980 and Universiti Pertanian Malaysia (Higher Degree) Regulations 1981. The Committee recommends that the candidate be awarded the relevant degree. Members of the Examination Committee are as follows:

Sidek Haji Abdul Aziz, Ph.D.

Associate Professor
Faculty of Science and Environmental Studies
Universiti Putra Malaysia
(Chairman)

Abdul Halim Shaari, Ph.D.

Professor
Faculty of Science and Environmental Studies
Universiti Putra Malaysia
(Member)

Zainal Abidin Talib Ph.D.

Associate Professor
Faculty of Science and Environmental Studies
Universiti Putra Malaysia
(Member)

Hishamuddin Zainuddin, Ph.D.

Associate Professor
Faculty of Science and Environmental Studies
Universiti Putra Malaysia
(Member)



GULAM RUSUL RAHMAT ALI, Ph.D.
Professor/Deputy Dean
School of Graduate Studies
Universiti Putra Malaysia

Date: 26 SEP 2003

This thesis submitted to the Senate of Universiti Putra Malaysia has been accepted as fulfillment of the requirement for the degree of Master of Science. The members of the Supervisor Committee are as follows:

Abdul Halim Shaari, Ph. D.

Professor
Faculty of Science and Environmental Studies
Universiti Putra Malaysia
(Chairman)

Zainal Abidin Talib Ph. D.

Associate Professor
Faculty of Science and Environmental Studies
Universiti Putra Malaysia
(Member)

Hishamuddin Zainuddin, Ph. D.

Associate Professor
Faculty of Science and Environmental Studies
Universiti Putra Malaysia
(Member)

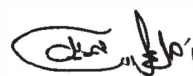


AINI IDERIS, Ph. D.
Professor/Dean
School of Graduatel Studies
Universiti Putra Malaysia

Date: '14 NOV 2003

DECLARATION

I hereby declare that the thesis is based on my original work except for quotations and citation which have been duly acknowledged. I also declare that it has not been previously or concurrently submitted for any other degree at UPM or other institutions.



ZOHRA ALI MOHAMED GEBREL

Date: 20/10/2023

TABLE OF CONTENTS

	Page
DEDICATION	.ii
ABSTRACT	iii
ABSTRAK	v
ACKNOWLEDGEMENTS	vii
APPROVAL	ix
DECLARATION	xi
LIST OF TABLES	Xiii
LIST OF FIGURES	xvi
LIST OF ABBREVIATIONS AND KEY WORD	xxiii
 CHAPTER	
I INTRODUCTION	1
Types of Magnetoresistance	1
Other types of Magnetoresistance are MR, TMR, EMR and VLMR	5
Application of CMR	7
Objective of the Study	9
 II LITERATURE REVIEW	 10
La _{1-x} Ca _x MnO ₃ System (LCMO)	14
Phase Diagram of La _{2/3} Ca _{1/3} MnO ₃	15
Doping effect on La Site	16
(La _{1-x} Tb _x) _{2/3} Ca _{1/3} MnO ₃ System (LTCMO)	17
(La _{1-x} Bi _x) _{2/3} Ca _{1/3} MnO ₃ System (LBCMO)	19
(La _{1-x} Dy _x) _{2/3} Ca _{1/3} MnO ₃ System (LDCMO)	19
(La _{1-x} Gd _x) _{2/3} Ca _{1/3} MnO ₃ System (LGCMO)	20
Jahn-Teller Effect	21
 III THEORY	 22
Introduction to Magnetism	22
Ferromagnetic	22
Antiferromagnetism	23
Néel Temperature (antiferromagnetic-ferromagnetic phase transition), T _N	23
Paramagnetism	24
Magnetic Susceptibility	26
Ferromagnetic Susceptibility	26
Curie-Weiss Law	27
Spin Glass	28
Double Exchange	29



	Jahn-Teller Effect	33
	Tolerance Factor	34
IV	SAMPLE PREPEARATION AND CHARACTERIZATION	37
	Preparation	37
	Chemical Powder Weighing	37
	Mixing	39
	Evaporation	39
	Calcinations	39
	Grinding and Sieving	40
	Pelleting	40
	Final Sintering	41
	Sample Characterization	43
	Resistance Measurement	44
	AC Magnetic Susceptibility Measurement	46
	Curie Temperature (ferromagnetic- Paramagnetic Phase transition), T_c	46
	Néel Temperature (antiferromagnetic -ferromagnetic phase transition), T_N	46
	Magnetoresistance Measurements	47
	X-Ray Diffraction Analysis	49
	Microstructure Analysis	.51
V	RESULTS AND DISCUSSIONS	55
	L _{1-x} Sn _x CMO system	55
	XRD Patterns and Lattice Parameters	56
	Susceptibility and Curie Temperature	56
	Effect of Frequency	58
	Effect of Field Intensity	64
	Resistance and Phase Transition Temperature, T_p	67
	Magnetic and Electrical Phase Diagram	69
	Microstructure Properties	70
	Magnetoresistance	76
	L _{1-x} Sm _x CMO system	85
	XRD Patterns and Lattice Parameters	85
	Susceptibility and Curie Temperature	98
	Effect of Field Intensity	91
	Phase Transition Temperature, T_p and Resistance	95
	Magnetic and Electrical Phase Diagram	97
	Microstructure Properties	98
	Magnetoresistance	104
	L _{1-x} Er _x CMO System	113
	XRD Patterns and Lattice Parameters	113
	Susceptibility and Curie Temperature	116
	Effect of Field Intensity	118
	Phase Transition Temperature, T_p and Resistance.	122
	Magnetic and Electrical Phase Diagram	124
	Microstructure Properties	126
	Magnetoresistance	132



VI	CONCLUSIONS AND SUGGETIONS	140
	Conclusions	140
	Suggestions	142
	REFERENCES	144
	APPENDICES	149
	BIODATA OF THE AUTHOR	180



LIST OF TABLES

Table		Page
1.1	Tyep of MR	6
4.1	Demagnetization factors, D (SI) for cylinders as a function of ratio of length to diameter, l/d	44
5.1	Lattice parameter, a, b, c and unit cell volume of Sn doped in LCMO system	55
5.2	Lattice parameter, a, b, c and unit cell volume of Sm doped in LCMO system	87
5.3	Lattice parameter, a, b, c and unit cell volume of Er doped in LCMO system	115



LIST OF FIGURES

Figures	Page
1.1 Temperature dependence of resistivity	7
2.1 Schematic structure of an ideal perovskite	11
2.2 Temperature dependence of resistivity of $\text{La}_{2/3}\text{Ba}_{1/3}\text{MnO}_3$ tin film at 0 and 5 T	12
2.3 Resistivity of $\text{Nd}_{0.5}\text{Pb}_{0.5}\text{MnO}_3$ as a function of temperature and magnetic fields	12
2.4 The phase diagram of $\text{La}_{2/3}\text{Ca}_{1/3}\text{MnO}_3$ system	16
3.1 Antiferromagnetic behavior of the sample	24
3.2 The atomic spin moment of (a) Ferromagnetic, (b) Antiferromagnetic and (c) Paramagnetic	25
3.3 Curie-Weiss law show the presence of paramagnetic phase	27
3.4 Schematic illustration of double exchange model	31
3.5 Sketch of the double exchange mechanism	32
3.6 A sketch of field splitting five-fold degenerate atomic 3d level into lower t_{2g} and higher e_g level...	34
3.7 phase diagram at constant doping $x=0.3$ as a function of tolerance factor	36
4.1 Sample preparation via solid-state reaction	38
4.2 Temperature setting for calcinations stage	42
4.3 Temperature setting for final sintering stage	42
4.4 Experiment rig for resistance measurement	43
4.5 Ac susceptometer Model 7000	46
4.6 Magnetoresistance measurement system	48
4.7 Schematic diagram of magnetoresistance measurement	49
4.8 Schematic illustration of fundamental processes in XRD measurement	50



4.9	Philips X-ray diffraction unit	51
4.10	Scanning Electro Microscope (SEM)	52
5.1	XRD Spectru for all the samples of LSnCMO system	56
5.2	Lattice parameter and unit cell volume of LSnCMO system	55
5.3	Temperature as a function of susceptibility of $(La_{1-x} Sn_x)_{2/3} Ca_{1/3} MnO_3$ with $x=0.0, 0.01, 0.02, 0.03, 0.04$ and 0.05 at frequency 125 Hz	57
5.4	Temperature as a function of susceptibility of $(La_{1-x} Sn_x)_{2/3} Ca_{1/3} MnO_3$ with $x=0.1, 0.2, 0.3$ and 0.4 at frequency 125 Hz	58
5.5	Temperature as a function of susceptibility of $(La_{1-x} Sn_x)_{2/3} Ca_{1/3} MnO_3$ with $x=0.1$ at frequency 200 Hz	59
5.6	Temperature as a function of susceptibility of $(La_{1-x} Sn_x)_{2/3} Ca_{1/3} MnO_3$ with $x=0.2$ at frequency 200 Hz	59
5.7	Temperature as a function of susceptibility of $(La_{1-x} Sn_x)_{2/3} Ca_{1/3} MnO_3$ with $x=0.3$ at frequency 200 Hz	60
5.8	Temperature as a function of susceptibility of $(La_{1-x} Sn_x)_{2/3} Ca_{1/3} MnO_3$ with $x=0.4$ at frequency 200 Hz	60
5.9	Spin glass temperature dependence of magnetic filed for LSnCMO with $x=0.2, 0.3$ and 0.4	61
5.10	Inverse susceptibility against temperature of LSnCMO system	63
5.11	T_c and Θ as a function of tin content of LSnCMO system	63
5.12	Susceptibility as a function of tin content at 80 K	65
5.13	Susceptibility as a function of tin content at 100 K	66
5.14	Susceptibility as a function of tin content at 150 K	66
5.15	Temperature dependence of resistance of LSnCMO system for samples with (a) $x=0.0, 0.03, 0.2$ and 0.3 (b) $x=0.01, 0.02, 0.04, 0.05, 0.1$ and 0.4	68
5.16	T_c and T_p as a function of tin content of LSnCMO system	69
5.17	SEM image of fracture surface of LSnCMO system	75
5.18	CMR curve of LSnCMO system as a function of applied magnetic field at 90 K	78



5.19	CMR curve of LSnCMO system as a function of applied magnetic field at 100 K	79
5.20	CMR curve of LSnCMO system as a function of applied magnetic field at 150 K	79
5.21	CMR curve of LSnCMO system as a function of applied magnetic field at 170 K	80
5.22	CMR curve of LSnCMO system as a function of applied magnetic field at 200 K	80
5.23	CMR curve of LSnCMO system as a function of applied magnetic field at 250 K	81
5.24	MR curve as a function of applied magnetic field of $(La_{1-x} Sn_x)_{2/3}Ca_{1/3}MnO_3$ with (a)x=0.0, (b)x=0.01, (c)x=0.02 and (d)x=0.05	83
5.25	CMR curve of LSnCMO system as a function temperature at 1.006 T	84
5.26	XRD patterns for the samples of $(La_{1-x} Sm_x)_{2/3}Ca_{1/3}MnO_3$ with x=0.0 to 0.4	86
5.27	Lattice parameter and unit cell volume of LSmCMO system	87
5.28	Temperature as a function of susceptibility of $(La_{1-x} Sm_x)_{2/3}Ca_{1/3}MnO_3$ with x=0.0, 0.01, 0.02 and 0.04	89
5.29	Temperature as dependence of susceptibility of $(La_{1-x} Sm_x)_{2/3}Ca_{1/3}MnO_3$ with x=0.03, 0.05, 0.1, 0.2, 0.3 and 0.4	89
5.30	Inverse susceptibility against temperature of LSmCMO system	90
5.31	T_c and Θ as a function of Samarium content of LSmCMO system	91
5.32	Temperature variation of A_c susceptibility for $(La_{1-x} Sm_x)_{2/3}Ca_{1/3}MnO_3$ with (a)x=0.03, (b)x=0.05, (c)x=0.1, (d)x=0.2, (e)x=0.3 and (f)x=0.4	94
5.33	Temperature dependence of resistance of LSmCMO system for samples with (a)x=0.0, 0.01 and 0.03 (b)x=0.0, 0.01, 0.02, 0.03, 0.04, 0.05, 0.1, 0.2, 0.3 and 0.4	96
5.34	T_c and T_p as a function of Samarium content of LSmCMO system	97
5.35	SEM image of fracture surface of LSmCMO system..	103
5.36	CMR curves of LSmCMO system as a function of applied magnetic field at 90 K	106



5.37	CMR curve of LSmCMO system as a function of applied magnetic field at 100 K	107
5.38	CMR curve of LSmCMO system as a function of applied magnetic field at 150 K	107
5.39	CMR curve of LSmCMO system as a function of applied magnetic field at 170 K	108
5.40	CMR curve of LSmCMO system as a function of applied magnetic field at 200 K	108
5.41	CMR curve of LSmCMO system as a function of applied magnetic field at 250 K	109
5.42	CMR curve as a function of applied magnetic field of $(La_{1-x}Sm_x)_{2/3}Ca_{1/3}MnO_3$ with (a)x=0.0, (b)x=0.01, (c)x=0.02, (d) x=0.03 and x=0.05	111
5.43	CMR curve of LSmCMO system as a function temperature at 1.006 T	112
5.44	XRD patterns for the samples of $(La_{1-x}Er_x)_{2/3}Ca_{1/3}MnO_3$ with x=0.0 to 0.4	114
5.45	Lattice parameter and unit cell volume of LErCMO system	115
5.46	Temperature as dependence of susceptibility of LErCMO system	117
5.47	Inverse susceptibility against temperature of LErCMO system	117
5.48	T_c and Θ as a function of erbium content of LSmCMO system	118
5.49	T_{SG} as a function of magnetic field	119
5.50	Temperature dependence of Ac susceptibility LErCMO system at different field intensity when (a)x=0.01, (b)x=0.02, (c)x=0.03, (d)x=0.04 and (f)x=0.05	122
5.51	Temperature dependence of resistance of LErCMO system for samples with (a)x=0.0, 0.01, 0.02, 0.03, 0.04 and 0.05 (b) x= 0.1, 0.2, 0.3 and 0.4	124
5.52	T_c and T_p as a function of Erbium content of LErCMO system	125
5.53	SEM image of fracture surface of LErCMO system	133
5.54	CMR curves of LErCMO system as a function of applied magnetic field at 90 K	134

5.55	CMR curve of LErCMO system as a function of applied magnetic field at 100 K	135
5.56	CMR curve of LErCMO system as a function of applied magnetic field at 150 K	135
5.57	CMR curve of LErCMO system as a function of applied magnetic field at 170 K	136
5.58	CMR curve of LErCMO system as a function of applied magnetic field at 200 K	136
5.59	CMR curve of LErCMO system as a function of applied magnetic field at 250 K	137
5.60	CMR curve as a function of applied magnetic field of $(La_{1-x}Er_x)_{2/3}Ca_{1/3}MnO_3$ with (a)x=0.01, (b)x=0.02 and (c)x=0.03	139
5.61	CMR curve of LErCMO system as a function temperature at 1 T	139



LIST OF ABBREVIATIONS AND KEY WORDS

T	Temperature in Kelvin
T_c	Curie temperature
T_N	Néel temperature
T_f	Freezing temperature
T_p	Phase transition temperature
T_{SG}	Spin freezing temperature
MR	Magnetoresistance
CMR	Colossal Magnetoresistance
GMR	Giant Magnetoresistance
AMR	Anisotropic Magnetoresistance
TMR	Tunnelling Magnetoresistance
EMR	Extraordinary Magnetoresistance
VLMR	Very Large Magnetoresistance
R (H)	The resistance in the magnetic field
R (0)	The resistance in zero magnetic field
DE	Double exchange
JT	Jahn-Teller
LCMO	La-Ca-Mn-O system
LSnCMO	La-Sn-Ca-Mn-O system
LSmCMO	La-Sm-Ca-Mn-O system
LErCMO	La-Er-Ca-Mn-O system
LTCMO	La-Tb-Ca-Mn-O system
LBCMO	La-Bi-Ca-Mn-O system
LDCMO	La-D-Ca-Mn-O system



LGCMO	La-Gd-Ca-Mn-O system
MI	Metal to insulator
MIT	Metal-insulator transition
AFM	Antiferromagnetic
AFI	Antiferromagnetic insulator
FMI	Ferromagnetic insulator
PMI	Paramagnetic insulator
$\langle A \rangle$	Average ionic radius
t	Tolerance factor
$d_{\text{La-O}}$	La-O bond distance
$d_{\text{Mn-O}}$	Mn-O bond distance
XRD	X-ray diffraction
SEM	Scanning Electron Microscope
H	Applied magnetic field
M	Magnetization
K_B	Boltzman constant
E_a	Activation energy
a, b, C	Lattice Parameter
hkl	Miller indices
d_{hkl}	Distance between atom and selected 2θ
χ	Susceptibility
Θ	Paramagnetic Curie point
f	Frequency
S	Spin electron
int	Intrinsic



CHAPTER I

GENERAL INTRODUCTION

Types of Magnetoresistance

Recently it has been discovered that certain types of materials exhibit extreme changes in electrical resistivity when a large magnetic field is applied. This effect, named as magnetoresistance is utilized in many types of sensors, measuring the amount and direction of magnetic fields. During the discovery of magnetoresistance, new effects found grew in strength and were progressively named anisotropic magnetoresistance (AMR), giant magnetoresistance (GMR), and colossal magnetoresistance (CMR), the latter being the main focus of this study (Valentine et al., 2002). The materials that exhibit CMR are manganate perovskites. In these materials the magnetoresistance arises from a difference in carrier scattering rates, depending on the relative orientation of the magnetization in the adjacent layers. The relative change in resistance, is usually defined as :

$$\frac{\Delta R}{R(0)} = \frac{[R(H) - R(0)]}{R(0)} \quad (1.1)$$

where $R(H)$ is the resistance at an applied field, and $R(0)$ is the resistance at zero field.